Frictional Properties of Red Pine Cones Harvested under Different Conditions

Yunze Ren, Chi Teng, Tong Gao, Ying Zhang, Hui Liu, and Xibin Dong *

* *Corresponding author: xibindong@nefu.edu.cn*

DOI: 10.15376/biores.19.1.766-788

GRAPHICAL ABSTRACT

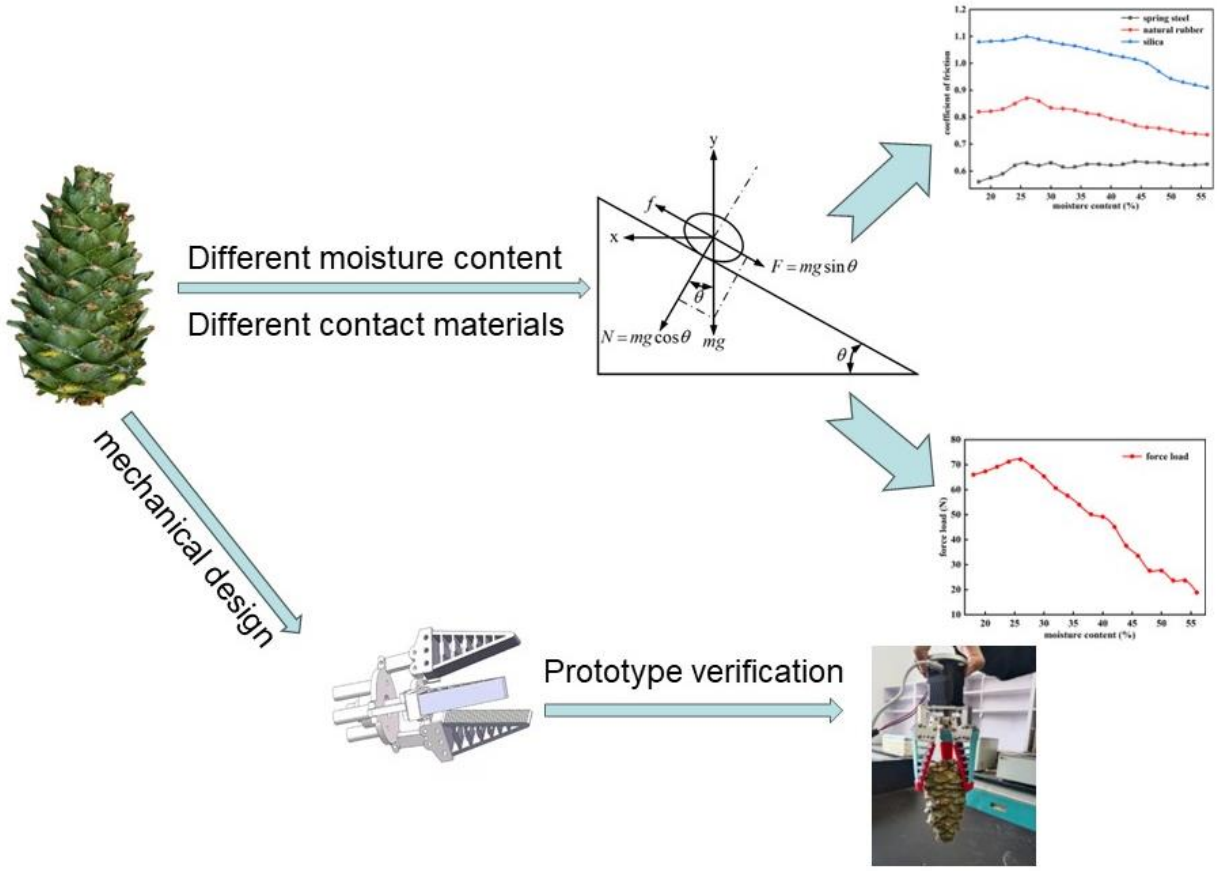

Frictional Properties of Red Pine Cones Harvested under Different Conditions

Yunze Ren, Chi Teng, Tong Gao, Ying Zhang, Hui Liu, and Xibin Dong *

The climbing of trees to pick pinecones is a high-risk exercise. In this study, a mechanical gripper jaw was designed. Frictional characteristics between the pinecones and the mechanical gripper jaw during pinecone picking under different conditions were investigated using a workbench simulation, homemade inclined friction meter, and mass tester. Three-level orthogonal and one-factor tests were conducted. The relationship between the water content and friction properties and between the water content and hardness were investigated, and conclusions were drawn on how water content affected friction properties by influencing hardness. The results showed that the contact material greatly affected the friction properties. The pinecone water content was maintained between 24% and 28% to ensure that the coefficient of friction was maximized and that the pinecones were sufficiently hard to dislodge. Additionally, a prototype machine was used to perform pinecone-gripping experiments to validate the experimental and simulation results. Consequently, the results of this study provide a useful reference for the structural design of pinecone picking robots and the picking reason.

DOI: 10.15376/biores.19.1.766-788

Keywords: Moisture content; Friction; Contact material; Orthogonal tests; Picking reason

*Contact information: College of Mechanical and Electrical Engineering, Northeast Forestry University, Harbin 150040, China; * Corresponding author: xibindong@nefu.edu.cn*

INTRODUCTION

The cones of red pines grow in clusters. When the cones are ripe, the pine nuts in them have high nutritional and medicinal value (Hou *et al.* 2021). With the large number of artificial reforestation efforts taking place in China, red pine cones can also be used as high-quality forest seeds; most artificial reforestation methods require the breeding of seedlings, and the demand for seeds has increased with the continuous growth of reforestation efforts (Liu *et al*. 2004). Consequently, it is important to realize efficient mechanized harvesting of red pine cones (Cui *et al*. 2023).

Pinecones generally grow at the top of pine trees, with pine tree heights being 10 to 15 m, and their crown width being 2 to 4 m. At this stage in China, most of the pinecone-picking methods involve manually carrying simple picking devices for picking operations, which usually require three steps. First, people (with the help of tools) climb to the upper parts of the trees; they then use bamboo poles or picking hooks and other tools to knock down the pinecones. Finally, other people collect the fallen pinecones (Wang *et al*. 2020; Li *et al*. 2021). During the picking process, the risks are high, efficiency is low, labor intensity is high, and the branches or trunks of the pine trees can be easily damaged by pinecones falling to the ground from great heights. Moreover, the pinecones can be

damaged. Therefore, it is essential to develop equipment that can replace the manual picking process (Bechar and Vigneault 2016).

In recent years, China has developed harvesting equipment including hydraulic lifting platforms, vibratory seed harvesters, and robots for collecting forest tree cones (Wu and Dong 2011; Zhang *et al.* 2021). However, the pinecone harvesting methods based on the design theory and methods of the key components of red pine cone harvesting are insufficient, as the extent of pinecone lignification is high, and their structural characteristics are complex. Consequently, these devices can only play an auxiliary role in the picking operation, and actual collection work still needs to be performed separately.

In recent years, research on the success of picking-type pinecone collection robots (which can cause irreversible damage to the branches and trunks of pine trees if poorly executed) has been limited. Clearly, picking pinecones should be similar to picking tomatoes, apples, and pears, and an appropriate mechanical gripper claw should be designed accordingly (Jiang *et al*. 2021). Osman Acar designed a four-link spherical mechanism to drive the gripper by a new method of measuring the curvature of the fingertip trajectory (Acar *et al*. 2021a). This gripper either compresses the object or wraps around an object when gripping it, with a high success rate of gripping (Acar *et al*. 2021b). However, the skin of pinecones is fish-scale-like and can fall off quite easily; therefore, the clamping mechanism used during the pinecone picking process should be precise. Consequently, the friction between the pinecone and the clamping mechanism is important and should be studied (Liu *et al.* 2021; Bu *et al.* 2022).

Research on the frictional properties of fruits and vegetables has focused on the mechanized harvesting of major plantation products, such as tomatoes, apples, kiwis, cucumbers, and maize. However, there is very little research on the mechanized harvesting of fruit and cones from large trees, especially on the frictional mechanical property requirements (Liu 2017; Tai *et al.* 2021; Li *et al.* 2022). Wei *et al.* (2020) studied the water content to determine the stress wave propagation velocity. Yu *et al.* (2017) studied the impact of moisture content on the mechanical properties of wood. Liu *et al*. (2023b) investigated the optimal way to harvest pinecones from a friction characteristics perspective using water content as a criterion. Other studies have proposed several methods to measure the friction coefficient, including the parallel wall, shear box, and inclined plane methods (Sun *et al.* 2018). Moreover, the coefficient of friction used in many harvesting equipment design studies has typically been measured using the slant method; the coefficient of friction measured using this method is simply the coefficient of sliding or rolling friction (Zhang *et al.* 2022).

Because the contact between the pinecone and friction material is made by protruding epidermal scales, different pinecone sizes can affect the quality, contact area, and epidermal contact hardness (Zhao *et al*. 2016). To study the friction characteristics between the end-effector jaws and pinecones in the process of pinecone picking, this study simulated the process using the ANSYS Workbench platform. The relationship between the pinecone size, pinecone moisture content, contact material, hardness, and the static friction and static coefficient of friction was examined using homemade slanting and texture gauges, taking the average value of each group of cyclic measurements 20 times. The experimental results were optimized to make a physical prototype, and its validity was demonstrated (Zhang *et al.* 2021). This study provides a reference for the design of pinecone picking equipment as well as methods to determine the friction characteristics and parameters.

EXPERIMENTAL

Materials

Pinecones taken from seed orchards in red pine forests in Jingpo Lake Xiaobeihu, Ning'an City, Mudanjiang, Heilongjiang Province, China. Spring steel (500 × 300 × 3 mm), rubber (500 × 300 × 3 mm), and silicone (500 × 300 × 3 mm) plates were used as contact materials. Freshly picked red pine cones were weighed in the forest to prevent water loss. The pinecones were then divided into three different grades—that is, large, medium, and small—based on the length and width of the cones, randomly numbered from 1 to 90 according to their grades and sealed and packed into a preservation box.

Fig. 1. The process of collecting red pine cones and their basic appearance

Instrumentation

Vernier calipers were used to measure the external dimensions of the pinecones. Selected red pine cones were then weighed using an HC-B 50002 electronic scale (range 5000 g, accuracy 0.01 g), and the 101-3AB electric blast drying oven (temperature 0 to 300 °C, voltage 220 V) was used to determine the pinecone moisture content. As shown in Fig. 2, a homemade friction coefficient inclinometer was used to determine the static friction coefficient, and the TexturePro CT V1.6 Build 26 texture analyzer was used to measure the hardness of the pinecone skin.

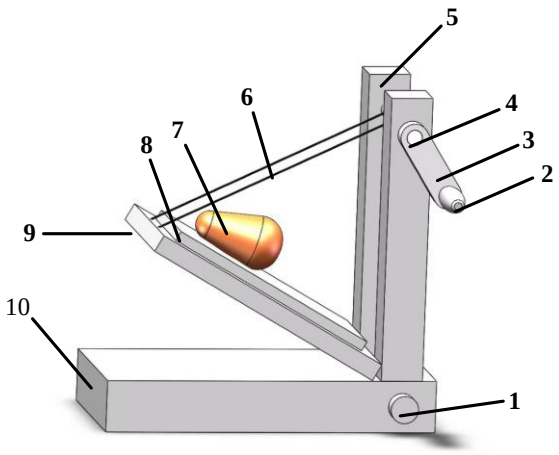

Fig. 2. Coefficient of friction inclinometer. 1. Articulating shaft; 2. Rocker; 3. Rocker arm; 4. Lifting shaft; 5. Bracket; 6. Lifting rope; 7. Sample; 8. Contact material; 9. Support frame; 10. Base

Principle

The static friction coefficient of the red pine cone was determined using the principle of hydrostatic friction. The red pine ball cone slides at the contact point of the contact material, so the coefficient of static friction was obtained using measurements of the friction angle. The force analysis of the red pine cone is as shown in Fig. 3. From the principle of static mechanics, in the red pine cone, the sliding moment force must satisfy Eq. 1, as follows,

$$f = F = mg \cdot sin\theta \quad (1)$$

$$F_N = mg \cdot cos\theta \quad (2)$$

$$f = \mu \cdot F_N \quad (3)$$

where θ denotes the angle of static friction (°), F denotes the component force in the direction of the inclined plane (N), f denotes the static friction (N), FN denotes the component force perpendicular to the inclined plane (N), f denotes the static friction (N), F_N denotes the component force perpendicular to the inclined plane (N), μ denotes the coefficient of static friction, m denotes the mass (kg), and g denotes the acceleration due to gravity (9.8 N/s^2).

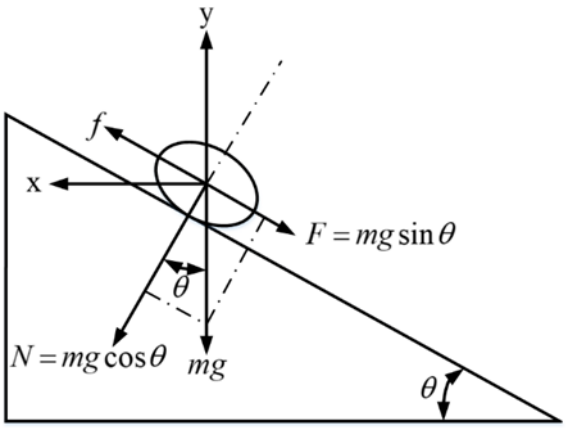

Fig. 3. Principle of friction coefficient measurement

The coefficient of static friction can then be calculated by Eq. 4.

$$\mu = f/F_N = mg \cdot sin\theta/mg \cdot cos\theta = tan\theta \quad (4)$$

Methodology and Content

To ensure suitable modeling of the picking robot and its subsequent gripping accuracy and stability, the geometric parameters of selected red pine cones were determined based on their classification. The shape of the red pine cone is approximately axisymmetric, so its maximum lateral width (L) and height (H) were selected as the values representing its external dimensions, and electronic vernier calipers (with an accuracy of 0.01 mm) were used to determine and calculate its geometric mean diameter using Eq. (5).

Sphericity refers to the closeness of the actual shape of the sample to a sphere. To facilitate the establishment of the proposed model, the sphericity (%) of the cones was calculated using Eq. (7) to determine the shape characteristics of the red pine cones, and their weight was measured using electronic scales, as follows,

$$d = (L \times H)^{\frac{1}{2}} \quad (5)$$

$$d_e = (L \times L \times H)^{\frac{1}{3}} \quad (6)$$

$$S_p = \frac{d_e}{d_c} \quad (7)$$

where d denotes the geometric mean diameter (mm), L denotes the horizontal maximum width (mm), H denotes the vertical height (mm), S_p denotes the sphericity (%), d_e denotes the diameter of a sphere equal to the volume of the actual object (mm), and d_c denotes the maximum diameter of the object (mm). The weight of the red pine cones m, maximum transverse width L, longitudinal height H, calculated geometric mean diameter d, and sphericity were measured, the results of which are shown in Table 1.

Table 1. Geometric Parameters and Quality of Red Pine Cones

	Mass (g)	Transverse width (mm)	Longitudinal height (mm)	Geometric Diameter (mm)	Sphericity (%)
Large	350.58	86.60	159.85	117.66	66.61
Medium	283.48	79.79	140.57	105.04	68.27
Small	197.70	75.15	116.46	93.45	74.89

With reference to the relative water content test method in GB/T 1931 (2009), three pinecones of different sizes were divided into three groups for the water content measurement test; pine oil on the surface of the pinecones was cleaned off and the three groups were weighed using an electronic scale. The test samples were then placed in a desiccator and heated at a controlled temperature of 103 ±2 °C for 24 h, and dried to absolute dryness (the boiling point of pine oil is 153 to 179 °C, so there was no effect on the pinecone quality). After drying, the test samples were weighed after being cooled to room temperature in a desiccator, and the water content of the red pine cones was calculated as follows,

$$\omega = (\rho^0 - \rho^1)/\rho^0 \quad (8)$$

where ω denotes the moisture content (%), ρ^0 denotes the fresh weight (g), and ρ^1 denotes the dry weight. With a measured pinecone moisture content of 25 to 50%, the samples were then baked to absolute dryness based on the moisture content being classified as 50 ± 3%, 35 ± 3%, and 20 ± 5%. Water of the required quality was stored in a sealed bag placed in an artificial climate chamber at 5 °C, and the sealed bag was turned twice daily to ensure that the water fully penetrated the pinecones. The pinecones were left to stand for 2 h before the actual moisture content parameters were determined.

Using controlled variable and orthogonal tests, the treated pinecones were placed on the friction coefficient inclinometer, which was in the plane at the initial position, to ensure that the tested pinecones were in full contact with the contact material. The ascending crank was slowly rotated to increase the inclination angle of the inclined plane, until the pinecones produced a micro-slip, at which point the crank was fixed, and the angle between the base and the contact material was recorded (Zhao *et al.* 2018), the value measured at this time being the pinecone static friction angle.

To minimize the effect of random error, one side of the pinecone was delineated as the fixed contact surface, the test was repeated 20 times, and the average value was taken to be the coefficient of static friction/static friction between the pinecone and the material under the selected conditions. Because the classical law of friction does not apply to soft elastic materials and the contact between the red pine cones and the material is dominated by the protruding contact of the fish-scale epidermis, the size of the pinecones influences the mass, contact area, and hardness of the epidermis in contact with the material; thus, the pinecone size is a critical factor. In large, medium, and small pinecones, contact was made with three different materials—namely, silicone, natural rubber, and spring steel—based on the different values of moisture content, to observe the effect of the three factors on the

coefficient of static friction/static friction. Consequently, a four-factor, three-level, multi-indicator orthogonal test was designed, using the factor levels as shown in Table 2 and the orthogonal test protocols as shown in Table 3.

Table 2. Orthogonal Test Factors and Levels

Level	Pinecone Size A	Contact Material B	Moisture Content C (%)	Empty Column D
1	Large	Silica	50% ± 3%	
2	Medium	Natural rubber	35% ± 3%	
3	Small	Spring steel	20% ± 3%	

Table 3. Orthogonal Test Protocols

Groups	Pinecone Size A	Contact Material B	Moisture Content C
1	1	1	1
2	1	2	2
3	1	3	3
4	2	1	2
5	2	2	3
6	2	3	1
7	3	1	3
8	3	2	1
9	3	3	2

Because the water content interval was set too large, to further explore the relationship between the pinecone water content and the coefficient of friction/static friction, a one-factor experiment was conducted, varying the water content from 56% to 20%, at 2% intervals with all other conditions remaining the same. Taking the large, medium, and small pinecone groups with different water content, the control of a single variable was used to explore the effect of water content on the coefficient of friction/static friction.

RESULTS AND DISCUSSION

Modeling and Simulation

Using the geometric parameters of the red pine cones listed in Table 1, the key part of the picking robot gripper was modeled, and force analysis of fingers was performed, as shown in Figs. 4 and 5.

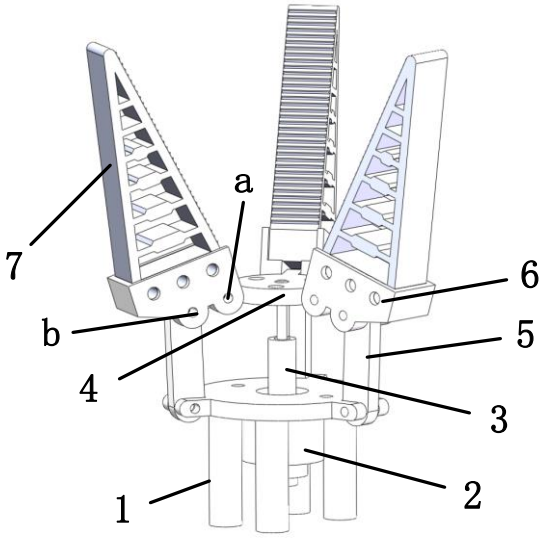

Fig. 4. Mechanical gripper model. 1. Base; 2. Electrical machinery; 3. Screw; 4. Transmission plate; 5. Support plate; 6. Claw-tip base; 7. Claw-tip; a. Connection point; b. Connection point

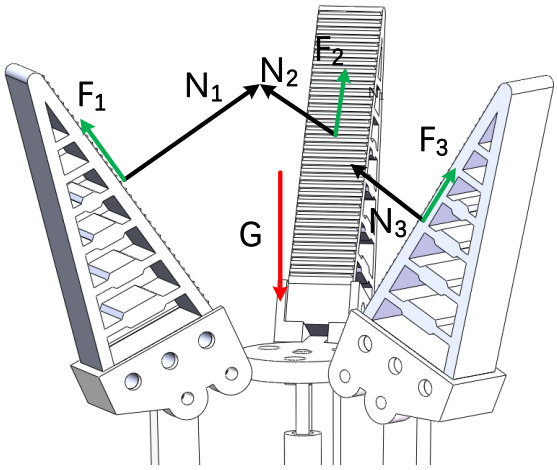

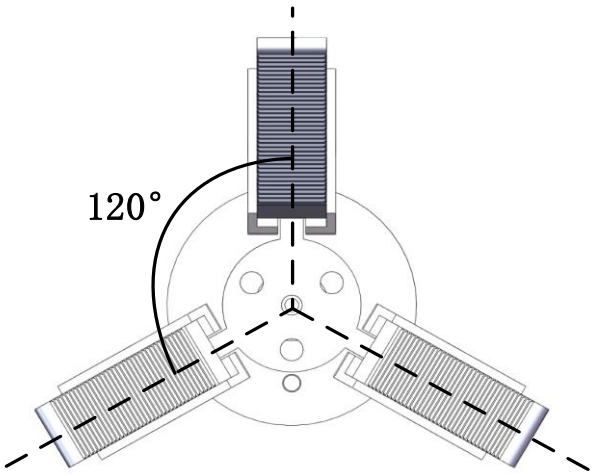

Fig. 5. Contact force between the mechanical gripper and the gripping object

By measuring the geometric size and quality of pine cones, the fixture size was designed with a maximum gripping diameter of 190 mm, and a 24V stepper motor was selected for driving to ensure gripping force. The structure of a mechanical claw consists of a base, motor, screw, transmission plate, claw tip base, support rod, and claw tip. The points in the figure represent the connecting heads of the transmission plate and the claw base, as well as the connecting heads of the claw base and the support plate. The opening movement of the mechanical claw is driven by the rotation of the motor, which drives the lead screw. The lead screw drives the transmission plate to raise itself, and the transmission plate drives the claw tip base to open outward. The closing motion of the mechanical claw is driven by the rotation of the motor, which drives the lead screw. The lead screw drives the transmission plate to lower itself, and the transmission plate drives the claw base to close inward. Due to the connection of the claw tip base to the support plate, the maximum angle formed between a single claw tip and the support plate is 120 °. During the grasping process, the mechanical claw generates a positive pressure perpendicular to the surface of the claw tip on the pine nut, and frictional force is generated between the pine nut and the claw tip. The combined force of frictional force, positive pressure, and the gravity of the pine nut itself are equal, but opposite in direction.

The main structure of the 3D printed mechanical claw used in the grasping process produces an arc-shaped bending deformation, realizing flexible grasping of the red pine cone and better protection of it to avoid damage; at the same time it increases the finger contact area, reduces the pressure, and ensures that the friction between the finger and the red pine cone can be increased by attaching three fingers of different materials. To increase the friction between the fingers and the pinecone, different materials (cut into serrated shapes) were attached to the inside of the three fingers, ensuring a more secure gripping action (Liu *et al*. 2021). Consequently, positive pressure and friction could be generated during the contact process between the flexible mechanical jaws and the target pinecone; moreover the positive pressure was always directed to the center of mass of the pinecone.

First, the software system Workbench 2020R2 was used to simulate the contact of a single finger and pinecone and the mechanical jaws grasping the pinecone, and to analyze the kind of deformation generated when the serrated structure of the finger surface and the

pinecone came into contact with each other, using different materials. Analysis of this deformation made it possible to determine which material was more suitable for increasing the friction between the contacting material and the pinecone. Three groups of tests were set up—that is, the 65 Mn spring steel, natural rubber, and silicone finger surfaces. The parameters of the finger surface materials and 3D printing material are shown in Table 4, and the simulation results are shown in Fig. 6.

Table 4. Material Property Parameters

Materials	Densities (kg/m^3)	Elastic Modulus (MPa)	Poisson's Ratio
Pinecone	550	9,000	0.4
65 Mn spring steel	7,810	196,500	0.3
Natural rubber	900	7.8	0.47
Silica	1,200	2.14	0.48
PLA	1,250	3,300	0.45

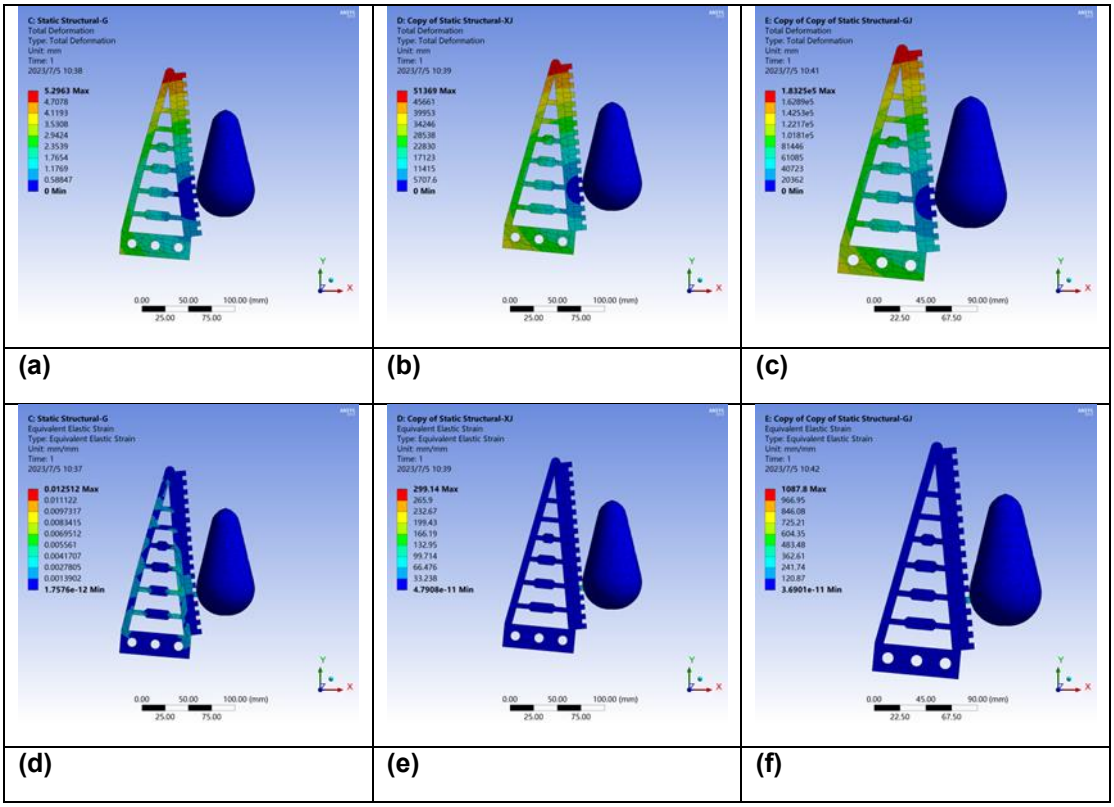

Fig. 6. Simulation results of the stress deformation using three distinct materials

Figures 6(a) and 6(d) show the total contact pressure and deformation cloud diagrams of spring steel, Figs. 6(b) and 6(e) show the total contact pressure and deformation cloud diagrams of natural rubber, and Figs. 6(c) and 6(f) shows the total

contact pressure and deformation cloud diagrams of silicone, where a pinecone with identical dimensions, load, and material properties was in contact with the three different materials. Deformation of the silicone was the largest, followed by natural rubber, and spring steel. The greater the stress and deformation generated at the contact area, the stronger the contact between the pinecone and the material; thus, the greater the friction generated to ensure that the pinecone can be successfully picked. To further investigate whether the simulation results were reasonable, orthogonal tests were designed to validate the simulation results.

Orthogonal Test

The conclusions drawn from the simulation and analysis of the simulated friction test scenarios indicated that the contact material had a significant effect on the friction coefficient. In the process of pinecone picking, the force exerted on the pinecone by the mechanical jaws and the friction between them (without destroying the structure of the pinecone itself) have an major influence on the success rate and efficiency of the pinecone picking process—that is, the friction force and coefficient are important parameters for describing friction in the picking process.

To study the degree of friction between the mechanical jaws and red pine cones under different conditions, orthogonal experimental parameters were used in accordance with the orthogonal test table, each group of tests being conducted 20 times. The results were averaged to observe changes in the friction force and coefficient of friction under different parameters, as shown in Table 5. The results of the orthogonal experimental results were subjected to analysis of variance (ANOVA), the results of which are shown in Tables 6 through 9.

Table 5. Orthogonal Test Program and Test Results

Groups	Pinecone Size A	Contact Material B	Moisture Content C	Friction f	Coefficient of Friction μ
1	Large	Silica	50% ±3%	2.45	0.93
2	Large	Natural rubber	35% ±3%	1.81	0.85
3	Large	Spring steel	20% ±3%	1.21	0.63
4	Medium	Silica	35% ±3%	1.56	1.02
5	Medium	Natural rubber	20% ±3%	1.12	0.80
6	Medium	Spring steel	50% ±3%	1.41	0.60
7	Small	Silica	20% ±3%	0.91	1.12
8	Small	Natural rubber	50% ±3%	1.12	0.74
9	Small	Spring steel	35% ±3%	0.75	0.58

Table 6. Extreme Variance Analysis of Friction using Three Factors

Factors	K_1	K_2	K_3	k_1	k_2	k_3	R	Preferred
A	5.47	4.09	2.78	1.82	1.36	0.93	2.69	A1
B	4.92	4.05	3.37	1.64	1.35	1.12	1.55	B1
C	4.98	4.12	3.24	1.66	1.37	1.08	1.74	C1

In Table 6, $K_i(i$=1,2,3) is the sum of all the results when the factor in its column is taken at level i. $k_i(i$=1,2,3) is the arithmetic mean of the results of all tests when the factor in its column is taken at level i. Therefore, $k_i = K_i/s$, where s denotes the number of levels of the factor; in this experiment, each factor is taken as three levels, s=3. The extreme deviation R is the difference between the maximum and the minimum k_i values in each column, $R = \max\{k_i(i$=1,2,3)$\} - \min\{k_i(i$=1,2,3)$\}$. Usually, the extreme difference of each column is not equal, indicating that the level change of each factor has a different impact on the test results; the larger the extreme difference, the greater the change in the value of the factor in the column within the test range, leading to the test indexes having a greater change in value. Consequently, the moment of the largest extreme difference is the factor level that has the greatest impact on the test results—that is, the most dominant factor. From the calculated polar deviation R in Table 6, the results show that the size of the pinecones has the greatest effect on friction, the size of the moisture content having the next largest effect, and the type of contact material having the smallest effect. Moreover, the test parameters producing the maximum static friction are large pinecones, silica gel, and 50% water content.

To further verify the accuracy of the orthogonal test analysis, the results were tested for significance of variance. The sum of squared deviations (S_j) reflects the difference in the test results caused by a change in the level of a factor,

$$S_j = \frac{(K_1)^2+(K_2)^2+(K_3)^2}{m} - \frac{\left(\sum_{i=1}^{n} y_i\right)^2}{n} \quad (9)$$

where $m = 3$, $n = 9$, and the total degrees of freedom $f_T = n - 1 = 8$. Individual factor degrees of freedom are $f_A = f_B = f_C = r - 1 = 3 - 1 = 2$, thus, the degree of freedom of the error is 2. The mean square is the quotient of the sum of squares of the deviations and the degrees of freedom. The F-value is the mean square of each factor/mean square error. By querying the F-quartile table, $F_{0.05}(2,2) = 19$, $F_{0.1}(2,2) = 9$.

The ANOVA results are shown in Table 7. The size of the pinecone had the greatest effect on friction, the moisture content had the next largest effect, and the type of contact material had the smallest effect. This is consistent with the ANOVA results and confirms the accuracy of the ANOVA. The size of the pinecone F exceeded $F_{0.05}(2,2) = 19$ proving that the size of the pinecones has a significant effect on the magnitude of static friction.

Table 7. Analysis of Variance of Three Factors on Friction

Source of variance	Sum of squared deviations	Degrees of freedom	Mean square	F	P	Significance
A	1.206288889	2	0.603144445	38.96841294	0.025019758	***
B	0.402422222	2	0.201211111	12.99999981	0.071428572	**
C	0.504622222	2	0.252311111	16.3015073	0.057798432	**
Errors	0.030955556	2	0.015477778	-	-	-
Sum	2.144288889	8	-	-	-	-

Table 8. Extreme Variance Analysis of Friction Coefficient by Three Factors

Factors	K_1	K_2	K_3	k_1	k_2	k_3	R	Preferred
A	2.41	2.42	2.44	0.80	0.81	0.81	0.03	A3
B	3.07	2.39	1.81	1.02	0.80	0.60	1.26	B1
C	2.27	2.45	2.55	0.76	0.82	0.85	0.28	C3

Table 8 presents the polar analysis of the three factors on the friction coefficient; the larger the polar difference, the greater the effect of the factor on the results. The order of magnitude of the extreme deviation was B > C > A—that is, the type of contact material had the greatest effect on the test results, followed by the moisture content, and the size of the pinecone. The test parameters that produce the maximum static coefficient of friction are small pinecones, silica gel, and a water content of 20%.

Table 9. Analysis of Variance of Three Factors on Friction Coefficient

Source of variance	Sum of squared deviations	Degrees of freedom	Mean square	F	P	Significance
A	0.000155556	2	0.000077778	0.013157932	0.98701295	-
B	0.265155556	2	0.132577778	22.42857143	0.042682927	***
C	0.013422222	2	0.006711111	1.135338346	0.468309859	*
Errors	0.011822222	2	0.005911111	-	-	-
Sum	0.290555556	8	-	-	-	-

To further verify the accuracy of the orthogonal test analysis, the results of the orthogonal test were tested for significance of variance, the results of which are presented in Table 9. The type of contact material had the greatest effect on the test results, followed by the water content. The size of the pinecones had the smallest effect, which is consistent

with the results of the ANOVA analysis and validates its accuracy. Based on the F-quantile table test, the contact material significantly affected the static friction coefficient.

The large pinecones and moisture content together affected the quality of the pinecones, which in turn affected the pressure generated on the contact material. When the pressure was too large, the static friction force was provided by the force in the direction of gravity, and effect of the type of contact material on the magnitude of static friction was not obvious. When studying the effect of test factors on the static friction coefficient, according to the theory of adhesive friction when the load is small, the two dyadic surfaces were in elastic contact. At this point, the actual contact area is proportional to the 2/3 power of the load, and the friction force was proportional to the actual contact area. Thus, the friction coefficient was inversely proportional to the 1/3 power of the load.

When the load was larger, the two dyadic surfaces were in elastic-plastic contact, and the actual contact area was proportional to the (2/3 to 1) power of the load. Therefore, the coefficient of friction decreased slowly with an increase in load and tended to stabilize. Moreover, the size of the static friction coefficient was related to the two pairs of surfaces under the action of the static contact over time.

In general, the longer the duration of static contact, the greater the coefficient of static friction. This is because of the action of the load, so that the contact plastic deformation (with the extension of the static contact time) increases the actual contact area, micro-peaks are embedded in each other, which is related to the depth (Liu *et al.* 2023).

Single-Factor experiment

The pinecones baked to absolute dryness were divided into 20 gradients ranging from 18% to 56% according to the moisture content grade at 2% intervals, and the samples were treated based on the same method used in the orthogonal test. To verify whether this test was in accordance with the theory of adhesion friction, the total number of test results was analyzed by linear regression using the R language, the results of which are shown in Tables 10 and 11.

Table 10. Linear Regression Analysis of Moisture Content on Frictional Force

Contact material	A linear regression equation	P	positive or negative correlation
Silica	$y = 2.43807x + 0.74021$	0	positive
Natural rubber	$y = 2.26372x + 0.60328$	0	positive
Spring steel	$y = 2.27159x + 0.37672$	0	positive

Table 11. Linear Regression Analysis of Moisture Content on Coefficient of Friction

Contact material	A linear regression equation	P	positive or negative correlation
Silica	$y = -0.376595x + 1.156659$	0	negative
Natural rubber	$y = -0.064362x + 0.818181$	0.0001487	negative

Spring steel	$y = -0.12925x + 0.66804$	0.04565	negative

The results obtained from Tables 10 and 11 and the linear fitting equations show that the moisture content had a positive effect on the friction force and a negative effect on the coefficient of friction. According to the theory of adhesive friction, the coefficient of friction is inversely proportional to the 1/3 power of the load, and the coefficient of friction is proportional to the contact area. Based on the results, this test is in accordance with the theory of adhesion friction.

Orthogonal tests show that the most significant factor affecting the friction force was the size of the pinecones, as different pinecone sizes have different masses and represent different loads. Therefore, to further explore the effect of the moisture content on the coefficient of friction, it was better to examine the three categories differently.

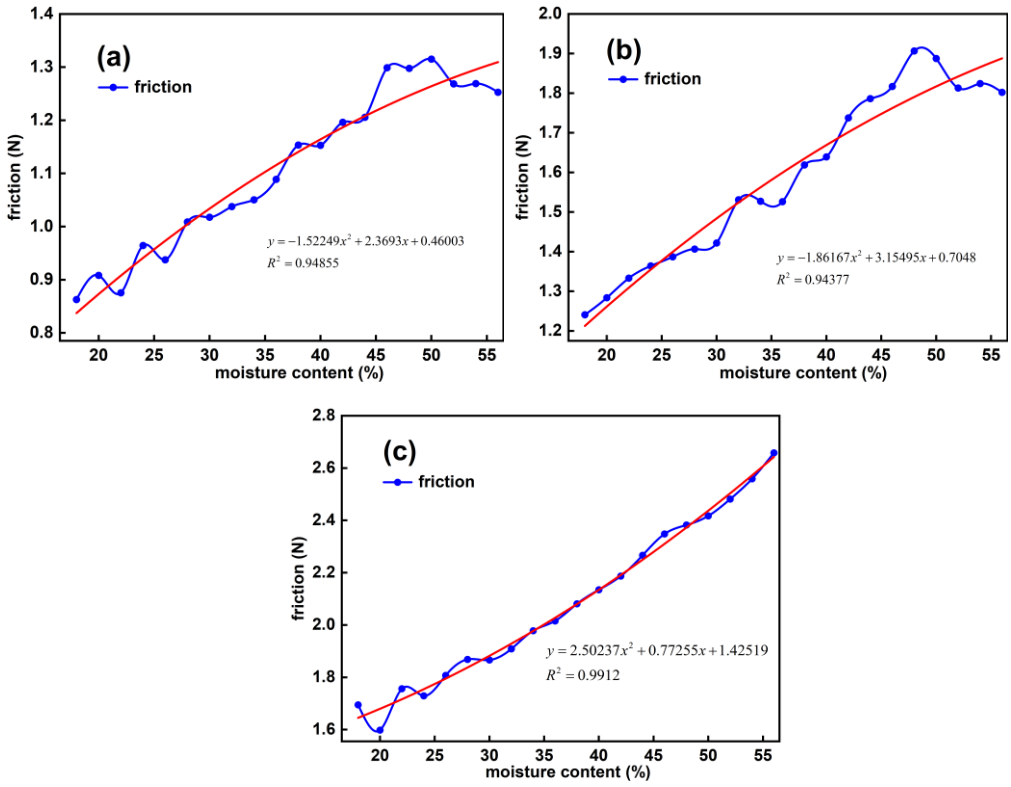

Fig. 7. Polynomial function curves for water content and friction

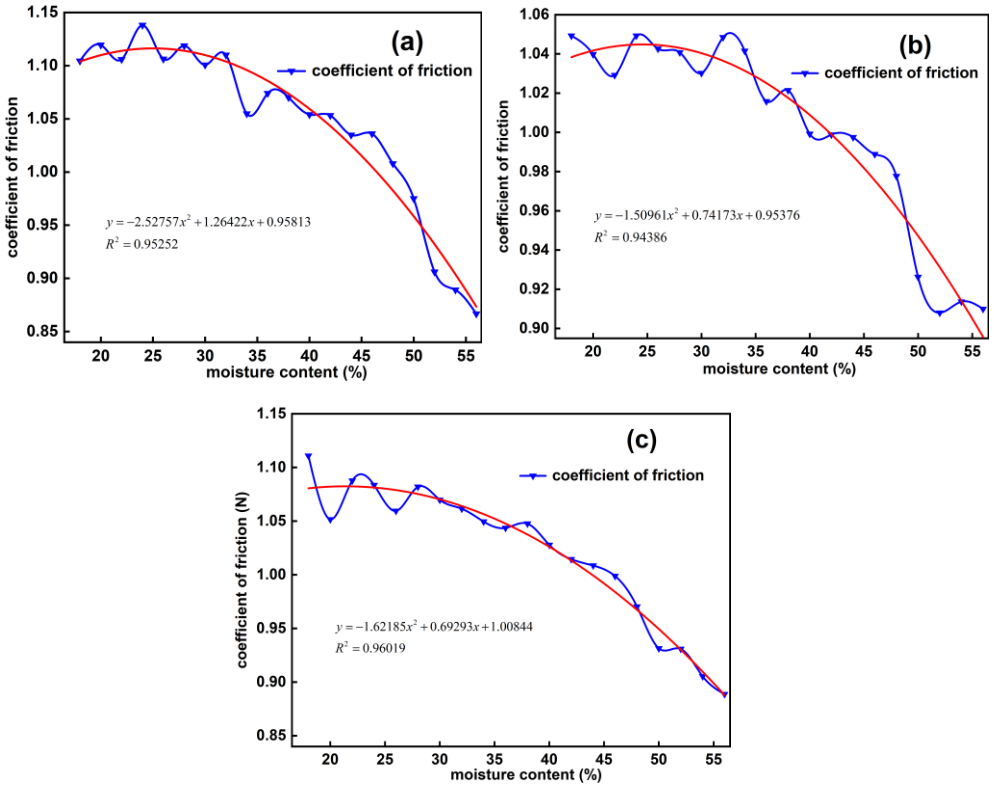

Fig. 8. Polynomial function curves of water content and coefficient of friction

For example, a significant factor affecting the coefficient of friction is the contact material. From the test results, the silicone material had a considerable advantage over the other materials, thus the small, medium, and large pinecone categories could be separated (using the letters A, B, and C), and different gradients of water content and silica gel material could be used for the test. The test results were repeated twenty times, and the average value was obtained. Because the volume of data was large, the gradient of the water content was used as a standard. The friction force and coefficient of friction were obtained by using the average value and Origin2022 fitted the polynomial function of the curves for the static friction and static coefficient of friction and water content, as shown in Figs. 7 and 8.

Figure 7 shows that the friction force increased gradually with the increase in water content (linearly); the effect of the increase was clear: it increased with increasing water content over time, and the function did not converge. In Fig. 8, the coefficient of friction first increased before decreasing with increasing water content. The fitted equations all exceeded 0.9, and the difference between the actual measured value and the predicted function value was small—that is, the fitting degree was high. The fitted polynomial equations show that the maximum values of the friction coefficients occurred when the moisture content was approximately 25%.

The analysis of this test showed that for static friction, the size and moisture content of the pinecones affected their quality, increasing the friction. The conditions affecting the static friction coefficient were as follows: first, the friction coefficient of the metal material was relatively low because the same metal (or the friction sub-metal of the metal with greater mutual solubility) is prone to adhesion, so that the coefficient of friction increases.

Additionally, the coefficient of friction is generally lower for different metals owing to their poor mutual solubility and adhesion. Second, owing to the presence of the surface film, the formation of a layer of oxide film in air reduces the coefficient of friction. Third, the effect of speed and temperature causes the molecules to change their state of motion. Fourth, a friction coefficient greater than 1 represents a friction angle exceeding 45°, which is caused by the prolongation of the static contact time, area of material contact, and different contact characteristics of the material itself—for example, the friction coefficient between indium and magnesium is 1.17, and the friction coefficient between indium and cadmium is 1.52. In determining the static friction coefficient of peanut pods under different water contents, Xu *et al*. (2022) concluded that their static friction coefficients with different contact materials under the same level of water content exhibited the same trend, increasing with the increase in water content.

The fitted quadratic function did not converge because the plasticity of peanut pods increased with an increase in water content, and the real contact area between peanut pods and material surfaces increased. First, as the plasticity of peanut pods increases with an increase in water content, the real contact area between the peanut pods and the material surface increases; however, when the water content increases, the adhesion between the them also increases, which increases the transverse shear force and net friction coefficient (Xu *et al.* 2022). In their study on the friction coefficient of cedar wood, Wang *et al.* (2018) found that it increased with increasing moisture content. Frodeson *et al.* (2019) concluded that the moisture content had a significant effect on the coefficient of friction of beech timber. As the moisture content increased, the coefficient of friction increased significantly; however, when the moisture content exceeded 30%, the increase was almost zero, the curve flattened out, and the coefficient of friction showed a segmental increase.

High water content had a negative effect on the friction coefficient. This is because the water content affects the surface roughness and hardness, and high water content lowers the hardness. The results obtained from this test are shown in Fig. 9.

The friction coefficients of the three contact materials were found to be very different from one another. For example, the friction coefficients of silica gel and natural rubber first increased, before decreasing with an increase in water content, except for the irregular change in the friction coefficient of spring steel, which exhibits an obvious convergence. By comparing the results of the above samples, it can be considered that because the contact between the pinecones and materials is via the surface fish-scale epidermis, the water content of pinecones not only affects the quality of the pinecones, but also affects their epidermal hardness and opening angle, which in turn affects the coefficient of friction by affecting the surface hardness. In response to this inference, a new set of one-way tests was designed to verify the relationship between pinecone hardness and moisture content.

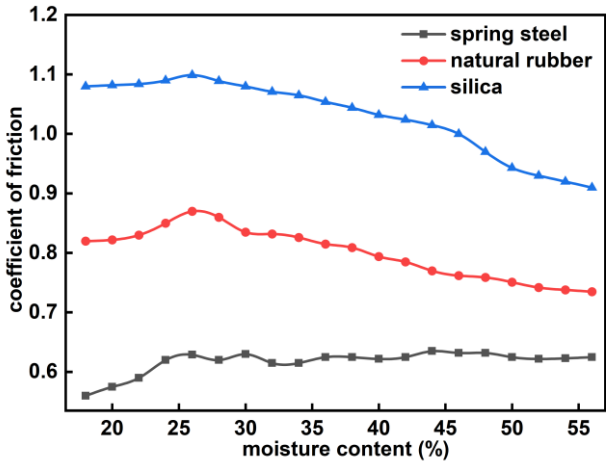

Fig. 9. Friction coefficients of three materials at different water contents

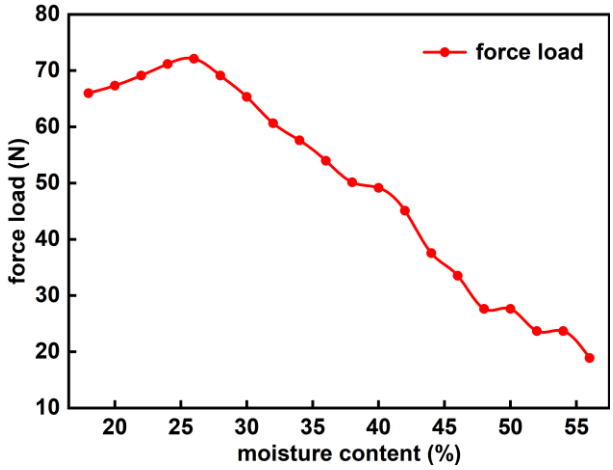

Fig. 10. Curve of water content versus surface hardness

The pinecones were oven-dried to absolute dryness and divided into 20 gradients based on the moisture content grade (from 18% to 56% in 2% intervals). The samples were treated in the same way as in the previous set of one-way experiments. The difference was that the three flattest pieces of skin on the surface of the pinecones were used as samples. They were trimmed into square blocks, which were then divided into the same water content gradients as in the previous set of experiments. The samples were fixed using a TexturePro CT V1.6 Build 26 texture analyzer, and a TA3/100 needle probe was used to conduct hardness tests on them. The samples were not distinguished between large and small; three pieces of epidermis were selected from each pinecone and each test was repeated five times, the average being taken, as shown in Fig. 10.

In Fig. 9, the force load applied by the texture analyzer on the pinecone epidermis first increased before decreasing with increasing water content. This indicates that the hardness of the pinecone skin showed a trend change with water content, first increasing and reaching a maximum value of approximately 25%, and then decreasing continuously; this is exactly the same as the trend of the total result plot of the coefficient of friction. Based on the theory of adhesive friction, the longer the static contact continuation time, the greater the static friction coefficient, owing to the effect of water content on the coefficient of friction. This is due to the action of the load, such that the plastic deformation of the contact (with the extension of the static contact time) increases the actual contact area, the micro-peaks being embedded in one another.

As natural rubber and silicone are soft elastic materials, the pinecone epidermis hardens, and the angle of tension is embedded in the contact material, thus increasing the contact area and coefficient of friction. When the water content changes, the surface hardness changes. However, between 18% and 30% water content, the measured force load changes were not large, indicating that when the water content reaches a certain value, the hardness remains constant. Moreover, the red pine cone skin angle also changes with changes in water content; however, when the water content is reduced, the skin angle of the pinecone increases as the change in skin angle also changes the contact surface area; consequently, the effect of the water content on the skin angle remains to be further validated.

Pinecone Picking Experiment

Based on the simulation results and experimental demonstration, by adjusting the dimensional parameters of the mechanical jaws, a pinecone picking mechanical jaw prototype was constructed, as shown in Fig. 9; a picking test was conducted in the laboratory environment. The structural material of the body of the mechanical jaws was the 3D-printed material PLA, and a layer of silica material was attached to the surface layer of the jaws.

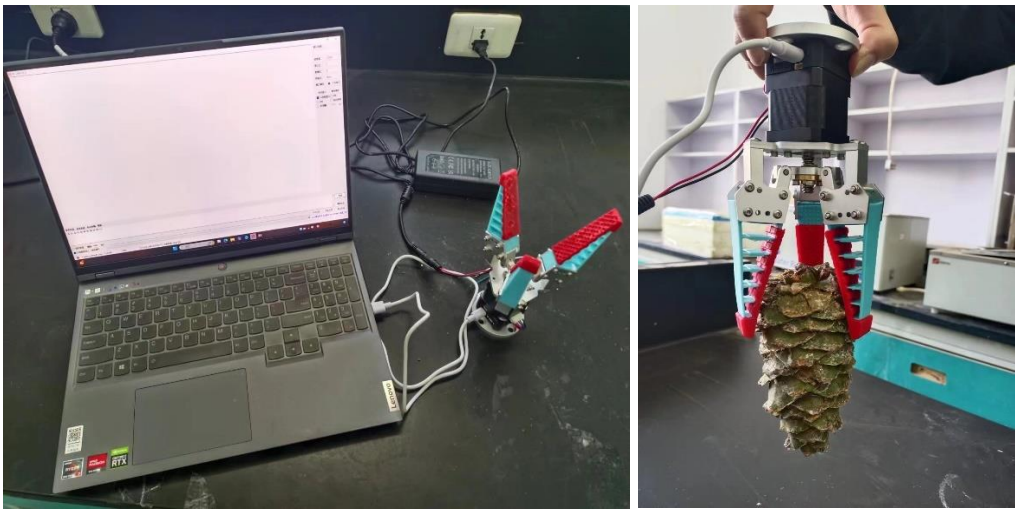

Fig. 11. Pinecone picking machine clamping jaws

In this study, the grasping success proportion and pinecone shedding proportion were used as the evaluation indices of the mechanical clip-grasping test, the formulas of which can be expressed as follows,

$$\eta_c = \frac{n_c}{N} \tag{10}$$

$$\eta_s = \frac{m_s}{n_c} \tag{11}$$

where η_c denotes the crawl success proportion, η_s denotes the pinecone abscission proportion, n_c denotes the number of successful grabs, m_s denotes the number of pinecone sheds, and N denotes the total number of grabs. Grasping experiments on the pinecones were conducted using a mechanical gripper jaw with silicone material as the finger surface, the test results of which are shown in Table 12. Three sets of trials were conducted and 48 tests were conducted on random pinecones.

Table 12. Pine Cone Grab Test Results

Groups	Total number of grabs	Number of successful crawls	Number of shedding	Crawl success rate	shedding rate
1	16	14	0	87.5	0
2	16	13	0	81.25	0
3	16	13	0	81.25	0
Sum	48	40	0	83.3	0

Based on an analysis of the test results, it was concluded that when silicone was used as the finger surface material, no pinecone shedding occurred; however, unsuccessful picking occurred. This is because there is a difference in the thicknesses of the individual pinecone stalks, which prevents them from being picked successfully when the clamping power is insufficient. Another problem that exists is the accumulation of wood resin during non-stop harvesting, and harvesting success is likely to be affected by the buildup of wood resin on the surface of the harvesting equipment jig during operation. In the current study, it was found that the lignocellulose resin is sticky and can make the friction between the pine cones and the fixture larger during the clamping process, which makes the fixture more secure when clamping the pine cones. However, the accumulation of the wood resin likewise had an effect on the opening of the jig. In future research, some tests could be conducted where a solvent is used to extract the wood resin and then a known amount of the solution could be applied to the surface of the fixture, followed by evaporation of all the solvent. This would be a quick way to obtain large amounts of wood resin on the surface of the manipulator. Additionally, reported testing was completed in a laboratory environment, while the pinecones are mostly grown in the upper part of red pine trees, which are subjected to wind, rain, and cold; consequently, there are differences in the actual pinecone picking conditions. The execution of this design is imperfect and needs to be optimized.

CONCLUSIONS

1. From the point of view of the friction coefficient, the silicone material exhibited a clear advantage, the moisture content being maintained between 24% and 28%, which ensured maximum surface hardness and produced the maximum coefficient of friction between the pinecone and the contact material.
2. The pinecone picking friction characteristics were investigated using a homemade inclined friction meter. The effects of various factors on the friction characteristics of pinecone picking were evaluated using a three-factor, three-level orthogonal test. The size of the pinecones, nature of the contact materials, and water content resulted in differences in the friction force and friction coefficient. To further investigate the relationship between the water content and friction characteristics, a one-way test was

conducted, and the skin hardness under different water content gradients was analyzed using a texture meter. The relationship between skin hardness and the coefficient of friction was explored, and a prototype machine was developed to further demonstrate the feasibility of the simulations and tests.

3. Different moisture content corresponds to different seasonal months, so the relevant content and related results could provide a reference for the design of pinecone picking end-effector structures, as well as new ideas for the pinecone-picking season.

ACKNOWLEDGMENTS

This study was supported by the Forestry Public Welfare Industry Research Special Program (Grant number 201504508).

REFERENCES CITED

Acar, O., Sağlam, H., and Şaka, Z. (2021a). "Measuring curvature of trajectory traced by coupler of an optimal four-link spherical mechanism," *Measurement* 176, article 109189. DOI: 10.1016/j.measurement.2021.109189

Acar, O., SağLam, H., and Şaka, Z. (2021b). "Evaluation of grasp capability of a gripper driven by optimal spherical mechanism," *Mechanism and Machine Theory* 166, 104486. DOI: 10.1016/j.mechmachtheory.2021.104486

Bechar, A., and Vigneault, C. (2016). "Agricultural robots for field operations: Concepts and components," *Biosystems Engineering* 149, 94-111. DOI: 10.1016/j.biosystemseng.2016.06.014

Bu, L., Chen, C., Hu, G., Sugirbay, A., Sun, H., and Chen, J. (2022). "Design and evaluation of a robotic apple harvester using optimized picking patterns," *Computers and Electronics in Agriculture* 198(No. C). DOI: 10.1016/j. compag.2022.107092

Cui, M., Lou, Y., Ge, Y., and Wang, K. (2023). "LES-YOLO: A lightweight pinecone detection algorithm based on improved YOLOv4-Tiny network," *Computers and Electronics in Agriculture* 205. DOI: 10.1016/j. compag.2023.107613

Frodeson, S., Henriksson, G., and Berghel, J. (2019). "Effects of moisture content during densification of biomass pellets, focusing on polysaccharide substances," *Biomass and Bioenergy* 122, 322-330. DOI: 10.1016/j.biombioe.2019.01.048

GB/T1931-1991(1991). "Methods for determining the moisture content of wood," Standardization Administration of China, Beijing, China.

Hou, D., Zhang, L., Wang, J. N., Li, J. Q., Zhao, C. H., Li, Z. X., and Zhang, H. G. (2021). "Variation in the cone, seed, and kernel nutritional components of *Pinus koraiensis*," *Silvae Genetica* 70(1), 205-216. DOI: 10.2478/sg-2021-0018

Jiang, J. Jia, Yuze Ye, Peilin Cheng, Runze Hu, and Chuanyu Wu (2021). "Design and parameter optimization of soft pneumatic gripper for slender fruits and vegetables picking," *Transactions of the Chinese Society for Agricultural Machinery* 52(6), 26-34. DOI: 10.6041/j.issn.1000-1298.2021–.06.003

Li, H., Yang, X., Yang, A., Yang, S., Zhang, Y., and Liu, J. (2021). "A specialized picker with lower pick-up height for recovering pruning residues in orchards," *Proceedings of the Institution of Mechanical Engineers, Part C: Journal of Mechanical Engineering Science* 235(23), 6908-6921. DOI: 10.1177/0954406221997495

Li Ma, Zhi He, Zhu Y, Wang Y, Li K (2022). "Design and experiment of dual manipulators parallel harvesting platform for kiwifruit based on optimal space," *Transactions of the Chinese Society for Agricultural Machinery* 53(8), 132-143. DOI:10.6041/j.issn.1000-1298.2022.08.014

Liu, Z.-G., Ji, L.-Z., Hao, Z.-Q., Zhu, J.-J., and Kang, H.-Z. (2004). "Effect of cone-picking on natural regeneration of Korean pine in Changbai Mountain Nature Reserve," *Chinese Journal of Applied Ecology* 15(6), 958-962. DOI: 10.13287/j.1001-9332.2004.0205

Liu, Z.-H. (2017). "Research progress analysis of robotic harvesting technologies in greenhouse," *Transactions of the Chinese Society for Agricultural Machiner*y 48(12), 1-18. DOI: 10.6041/j.issn.1000-1298.2017.12.001

Liu, X.-M., Tian, D., Song, M., Geng, D., and Zhao, Y. (2021). "Design and experiment on pneumatic flexible gripper for picking globose fruit," *Transactions of the Chinese Society for Agricultural Machinery* 52(2), 31-43. DOI: 10.6041/j.issn.1000-1298.2021–.02.003

Liu, S., Liu, M., Liu, T., Xiao, H. and Xiao, B. (2023a). "Wear characteristics of brazing diamond abrasive wheels for high-efficiency grinding of ferrous metals," *Wear* 514-515. DOI: 10.1016/j.wear.2022.204580

Liu, W., Chen, M., Liu, H., Yi, B., Hu, H., Zhang, Y., Liu, D., and Li, C. (2023b). "Isothermal drying characteristics and kinetic mechanism for tobacco with different water content," *BioResources* 18(2), 2611-2625. DOI: 10.15376/biores.18.2.2611-2625

Luo, Y. Y., Xiao, S. L., and Li, S. L. (2017). "Effect of initial water content on foaming quality and mechanical properties of plant fiber porous cushioning materials," *BioResources* 12(2), 4259-4269. DOI: 10.15376/biores.12.2.4259-4269

Sun, J., Ji, Z., and Ma, C. (2018). "Reanalysis of the contact mechanics for rough surfaces," *Chinese Journal of Theoretical and Applied Mechanics* 50(1), 68-77. DOI: 10.6052/0459-1879-17-272

Tai, H. L., Guan, Y, Ding, N., Du, Y, Mao, E. (2021). "Simulation of a maize ear picking device with a longitudinal horizontal roller based on hypermesh modeling," *BioResources* 16(1), 1394-1410. DOI: 10.15376/biores.16.1.1394-1410

Wang, H. Q., T, H. T., Feng, C., and Qian, J. (2018). "Effect of moisture content and angle between fiber and wood axial direction of *Cunninghamia lanceolata* on surface roughness and friction coefficient," *Journal of Zhejiang Forestry Science and Technology* 38(4), 61-65. DOI: 10.3969/j.issn.1001-3776.2018.04.010

Wang, K.-Q., Zhang, W.-H., Luo, Z., and Zhang, Y.-H. (2020). "Design and experiment of hitting pinecone picking robot," *Transactions of the Chinese Society for Agricultural Machinery* 51(8), 26-33. DOI: 10.6041/j.issn.1000-1298.2020.08.003

Wei, X., Sun, L., Zhou, H., Yang, Y., Wang, Y., and Gao, Y. (2020). "Propagation velocity model of stress waves in larch wood (*Larix gmelinii*) three-dimensional space with different moisture contents," *BioResources* 15(3), 6680-6695 DOI: 10.15376/biores.15.3.6680-6695

Wu, H., and Dong, X. (2011). "Research progress in tree seed harvesting technology and equipment," *Forest Engineering* 27(4), 24-29. DOI:10.16270/j.cnki.slgc.2011.04.015

Xu, X., Yan, J., Wei, H., Bao, G., Ji, L., and Xie (2022). "Determination of static friction coefficient of peanut pod under different moisture content," *Journal of Chinese Agricultural Mechanization* 43(2), 93-97. DOI: 10.13733/j.jcam.issn.2095-5553.2022.02.013

Zhang, P., H. Xu, X. Zhuo, Z. Hu, C. Lian and B. Wang (2022). "Biotribological characteristic of peanut harvesting impact-friction contact under different conditions," *Agronomy* 12(6). DOI: 10.3390/agronomy12061256

Zhang, S., Wang, Z., Wang, L., Liu, S., Zhang, Y., Miao, H., Dai, M., and S. Liu, S. (2021). "Design and experimental study of ginkgo leaf picking device," *Proceedings of the Institution of Mechanical Engineers, Part C: Journal of Mechanical Engineering Science* 235(24), 7353-7362. DOI: 10.1177/09544062211023118

Zhao, N., Meng, P., and Yu, X. (2018). "Photosynthetic stimulation of saplings by the interaction of CO_2 and water stress," *Journal of Forestry Research* 30(4), 1233-1243. DOI: 10.1007/s11676-018-0764-9

Zhao, Y., Gong, L., Huang, Y., and Liu, C. (2016). "A review of key techniques of vision-based control for harvesting robot," *Computers and Electronics in Agriculture* 127, 311-323. DOI: 10.1016/j.compag.2016.06.022

Article submitted: July 28, 2023; Peer review completed: September 2, 2023; Revised version received and accepted: October 5, 2023; Published: December 8, 2023.
DOI: 10.15376/biores.19.1.766-788